



Delft University of Technology

Estimation of Flight State with a Collision Alert Radar Based on FMCW Reflections of the Landscape for General Aviation

Maas, J.B.; van Gent, R.N.H.W.; Hoekstra, J.M.

Publication date

2020

Document Version

Final published version

Published in

ICRAT 2020

Citation (APA)

Maas, J. B., van Gent, R. N. H. W., & Hoekstra, J. M. (2020). Estimation of Flight State with a Collision Alert Radar Based on FMCW Reflections of the Landscape for General Aviation. In *ICRAT 2020*

Important note

To cite this publication, please use the final published version (if applicable).
Please check the document version above.

Copyright

Other than for strictly personal use, it is not permitted to download, forward or distribute the text or part of it, without the consent of the author(s) and/or copyright holder(s), unless the work is under an open content license such as Creative Commons.

Takedown policy

Please contact us and provide details if you believe this document breaches copyrights.
We will remove access to the work immediately and investigate your claim.

Estimation of Flight State with a Collision Alert Radar

Based on FMCW Reflections of the Landscape for General Aviation

Jerom Maas

TU DELFT

Faculty of Aerospace Engineering
Control and Simulation department

Delft, Netherlands

j.b.maas@tudelft.nl

Ronald van Gent

Selfly BV

Soest, Netherlands

Jacco Hoekstra

TU DELFT

Faculty of Aerospace Engineering
Control and Simulation department

Delft, Netherlands

Abstract—Although the main goal of a newly developed Collision Alert Radar is to observe airborne targets, it was found that reflections of the ground are received by the radar. The radar is carried on board of the aircraft, and the ground reflections may be used to detect flight information with respect to the terrain, something which is not possible with existing hardware.

In this paper a method is developed which makes use of range and Doppler information from ground reflections, in order to provide the pilot with height and velocity information. The method was tested on a local flight in the Netherlands, with a prototype of the radar on-board. State results were compared to those of a GPS tracker on board.

It was found that the horizontal and vertical components of the velocity were found with a standard deviation of about $3m/s$, and the height estimates had a standard deviation of $23m$. Also, a discrepancy of $36m$ between the GPS and radar height estimates was found, which was caused by a fault in the GPS earth surface model, which was no problem for the radar.

It is concluded that the quality of radar state estimates is approaching that of GPS measurements. The rapid developments in microwave sensing techniques can help the radar to surpass the quality of GPS in the coming years. If that happens, state estimation by radar can become an option for pilots who do not want to be dependent on the correctness of a terrain model, but who measure the terrain shape independently.

Radar; Sense and Avoid; Collision Alert; FMCW; GPS; General Aviation; Height; Altitude; Ground Speed; Climb Rate

I. INTRODUCTION

An airborne Collision Alert Radar is being developed for use in General Aviation (GA). Although its primary goal is not to detect the ground, reflections from the surface are observed in the radar output. These reflections can contain useful information for a GA pilot, since it is crucial to know the aircraft state with respect to the landscape.

The traditional flight instruments of an aircraft provide the pilot with the state information by interpreting the air data. Inertial Navigation Systems (INS) track the aircraft position by Dead Reckoning from take-off. Navigation on the hand of GPS is used in commercially available navigation apps. None of these instruments measure the surface, but the position of the ground is stored in an internal model of the elevation. But this map may be outdated or lack detail, or temporary obstacles such as cranes may be missing. Such faults can lead to unsafe situations.

In order not to rely on an elevation map, it is possible to perform direct measurements on the surface. This can be done with a radar or LIDAR altimeter [1]. These systems measure the distance to the ground directly below the aircraft. This provides information from a single point and not about the entire landscape. For collision warnings about the landscape in front of the aircraft, the pilot is still dependent on an internal elevation model. The limited functionality of LIDAR altimetry, combined with a steep price, is the reason that LIDAR altimeters are not often used in GA.

Progress in the field of microwave sensing has empowered the development of new portable radar hardware for direct measurements. Such a new system can be used in GA, as a Collision Alert Radar. Example functionalities are to detect wind turbines and to track aircraft in 3D. The equipment will cost less than a complete ADS-B/CDTI combination, and all ‘sense and avoid’ functions can be performed simultaneously by a single machine. The application of portable radar in GA looks promising, and the processing methods for it are being developed.

In this paper, the development and testing are presented to use reflections of the Collision Alert Radar to determine the state of the aircraft with respect to the landscape. This method makes

use of the wide aperture of the radar, as well as the signal filtering properties. The method combines several surface reflections in front of the aircraft into one final aircraft state, and can therefore provide ground collision warnings based on the landscape in front of the aircraft. This is not possible with existing equipment.

The underlying hardware and software principles of the state determination method are presented in chapter II. The radar and the algorithm are subjected to a flight test, which is presented in chapter III. The results of the flight are presented in chapter IV, and a discussion on these is found in chapter V. Conclusions on the algorithms are given in chapter VI.

II. METHOD

In this chapter the method for detecting the state is introduced. The hardware and software are described in the first and second parts. The final section of the chapter contains a computer simulation experiment, which is used to verify the method.

A. Hardware

The development of self-driving cars has caused a significant improvement of the quality and the price of modern sensor hardware and software [2][3][4]. Because of this, new systems can be developed which complement the shortcomings of current flight instruments [5].

Frequency modulated continuous-wave (FMCW) radar systems measure range and Doppler velocity of objects in sensor range [6]. The weight, cost, and power consumption are low enough that they can be taken on board of a small aircraft, and be used to sense the aircraft surroundings [7][8].

A Collision Alert Radar system is developed for use in GA. The system is developed to have a wide aperture, up to *60degrees* horizontally and vertically. Other aircraft can be seen with these radars, and ground reflections are observed as well.

An FMCW radar system can measure both the distance to and the Doppler velocity of an object [2][6], after antialiasing is performed [9][10]. The Doppler velocity is the component of the relative velocity in the distance direction. Direction of Arrival Estimation can help localize a source of reflection in three dimensions [11][12].

When the radar system is moving over a landscape, the surface can be seen as a collection of objects with different distances and relative radial velocities. The measured signals can be used to determine the instantaneous state of the system.

B. Software Model

The landscape is modelled as an inertial flat plane which reflects emitted radar signals back to the system. Since the

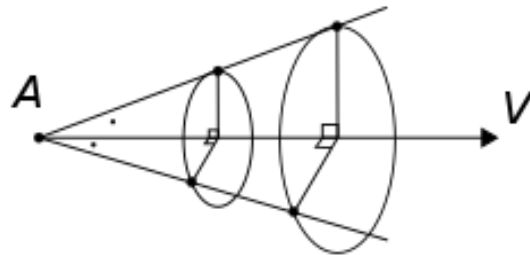


Figure 1: Aircraft A and four points with the same angle between distance and velocity vector forming a cone

surface is not moving, the relative velocity vector is equal at all locations on the surface.

Radial velocity is defined as the component of the relative velocity vector in distance direction [10]. Since the relative velocity is the same everywhere, this is only dependent on the angle between the distance and velocity vectors of a point.

This means that two points will have an equal radial velocity only if the angles between their distance vectors and the aircraft velocity vector are equal to each other. As illustrated in Figure 1, this means that all points with the same radial velocity must lie on a three-dimensional cone around the system velocity vector.

A contour plot on the surface is created, connecting the points on the surface with equal radial velocity. Since all such points must lay on the three-dimensional cone and on the surface plane, the resulting curves are hyperbolas, parabolas and ellipses. The transverse axes of the hyperbolas are the projection of the axis of the cones, i.e. the aircraft velocity vector. A second contour plot is added to the figure, connecting

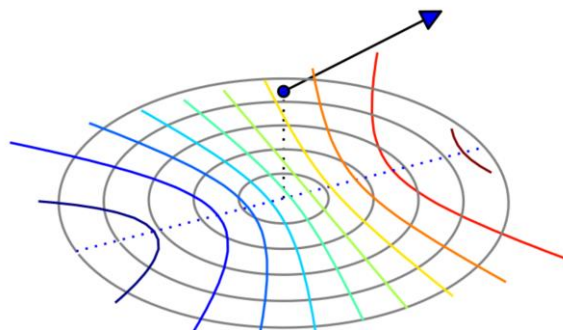


Figure 2: 3D view of a system with a velocity above a flat surface, with contour plots of equal distance (grey) and equal radial velocity (colours)

surface elements with the same distance to the system. The result is seen in Figure 2.

From Figure 2 it is observed that for a given distance to the system, multiple radial velocities exist. For this given distance, the maximal and minimal radial velocities can be found where the hyperbolas are tangent to the circle. Since the center of this circle lies on the transverse axes of the hyperbolas, the two types of contour plots must be tangent at the vertices of the hyperbolas, which is indicated as the dotted line in the figure.

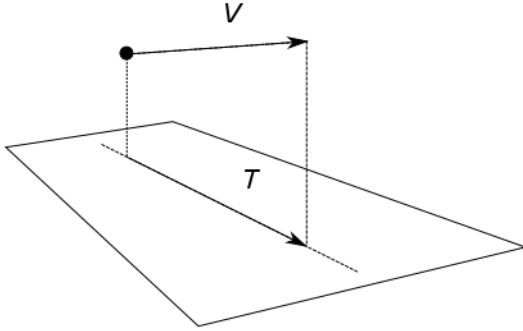


Figure 3: 3D view of the track vector T as the projection of the velocity V on the ground

This means that for a given distance to the system, the maximal and minimal radial velocities can be found at the transverse axis of the hyperbolas. This axis is the projection of the system velocity vector on the plane, which will be called the track vector. The track vector is illustrated in Figure 3.

The FMCW radar can measure the distance and radial velocity of all points that form the surface. It is now found that:

For a given distance, the surface points with the maximal and minimal radial velocities must lay on the track vector of the radar system.

This is also given in mathematical notation. Say S is the collection of points p on the surface, and V is the velocity vector of the aircraft. Note $V_r(p)$ and $r(p)$ as the Doppler velocity and the range of p . Then it follows:

$$\begin{aligned} S &= \{p: p \text{ on surface}\} \\ S_x &= \{p: p \in S, r(p) = x\} \\ T &= \{p: p \in S, p \text{ below } V\} \\ p \in T &\leftrightarrow V_r(p) = \max\{V_r(s): s \in S_{r(p)}\} \end{aligned} \quad (1)$$

a) State Finding Theory

In Figure 4 a side view is given of a radar system above a surface. According to the theorem in the previous section, point P is the point with the highest radial velocity V_R of all measurements with distance r .

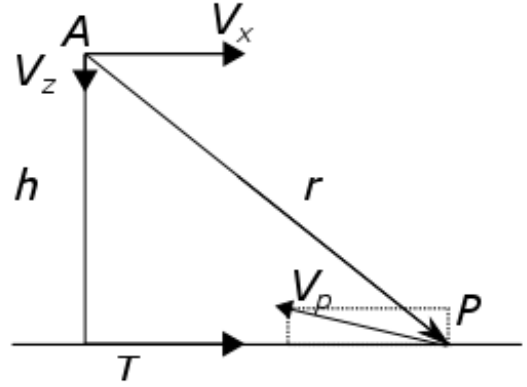


Figure 4: Side view of the geometry between a moving aircraft A and a point P on the track vector T

The radar system moves with a velocity of V_S . This means that the relative velocity vector of P is given as:

$$\vec{V}_P = -\vec{V}_S = \begin{bmatrix} -V_x \\ -V_z \end{bmatrix} \quad (2)$$

The radial velocity (which is measured), is a component of this relative velocity vector:

$$V_r = \frac{\vec{V}_P \cdot \vec{r}}{r} = \begin{bmatrix} -V_x \\ -V_z \end{bmatrix} \cdot \begin{bmatrix} \sqrt{r^2 - h^2} \\ h \end{bmatrix} \frac{1}{r} \quad (3)$$

This equation is written out in the following way:

$$\begin{aligned} V_r \cdot r + V_z \cdot h &= -V_x \sqrt{r^2 - h^2} \\ (V_r \cdot r)^2 + 2V_r r V_z h + (V_z \cdot h)^2 &= V_x^2 (r^2 - h^2) \\ (V_r \cdot r)^2 + 2V_r r V_z h + h^2 (V_x^2 + V_z^2) &= r^2 V_x^2 \\ \frac{1}{V_x^2} (V_r \cdot r)^2 + \frac{2V_z h}{V_x^2} V_r r + \frac{h^2}{V_x^2} (V_x^2 + V_z^2) &= r^2 \end{aligned}$$

With multiple measurements of V_r and r , a set of equations can be constructed:

$$\begin{bmatrix} (V_{r_0} r_0)^2 & V_{r_0} r_0 & 1 \\ (V_{r_1} r_1)^2 & V_{r_1} r_1 & 1 \\ \dots & \dots & \dots \\ (V_{r_n} r_n)^2 & V_{r_n} r_n & 1 \end{bmatrix} \begin{bmatrix} a \\ b \\ c \end{bmatrix} = \begin{bmatrix} r_0^2 \\ r_1^2 \\ \dots \\ r_n^2 \end{bmatrix} \quad (4)$$

With the parameters:

$$\begin{aligned} a &= \frac{1}{V_x^2} \\ b &= \frac{2V_z h}{V_x^2} \\ c &= \frac{h^2}{V_x^2} (V_x^2 + V_z^2) \end{aligned}$$

The equation is now in the form $AX=B$, with matrices A and B only containing measured data: V_r and r . The other three terms, a , b and c consist of combinations of V_h , V_z and h . These are unknown parameters, and they describe the state of the radar system: the velocities tangential and perpendicular to the landscape, and the height above it. If at least three surface points are observed, a least squares solution to the equation can be found and parameters a , b and c are known. Observing more points p increases the accuracy of the a , b and c parameters. The aircraft state can then be computed as follows:

$$V_x = \sqrt{\frac{1}{a}} \quad (5)$$

$$V_z = \frac{b}{\sqrt{4a^2c - ab^2}} \quad (6)$$

$$h = \sqrt{c - \frac{b^2}{4a}} \quad (7)$$

The challenge is to observe multiple suited surface points with values of V_r and r . Therefore, the reflections that lay on the track vector must be distinguished from the rest. This can be done in several ways, for example with Direction of Arrival Estimation [11][12]. In this paper (1) is used, as introduced previously.

Using this theorem means that if all observed reflections are sorted in range bins [13], the track vector can be found by selecting the observation with the highest value for V_r . This will provide a set of data points with different values of r and V_r , and with this it is possible to compute the aircraft state.

C. Verification by Simulation

The method presented in this section is first subjected to a verification run in a simulation. A virtual flight is performed in the X-plane simulator. Radar output was generated by simulation as well. Results of the altitude estimates are seen in Figure 5.

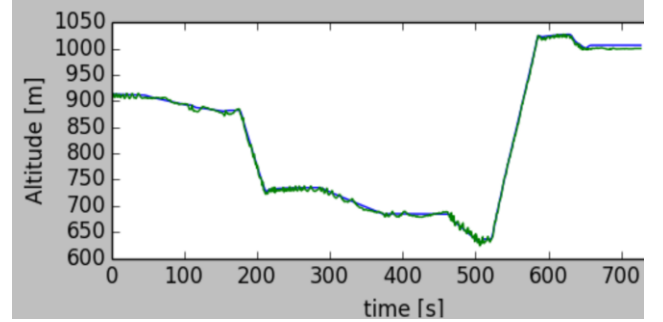


Figure 5: Simulation results of flight altitude (blue line) and method results (green line)

In Figure 5 it is seen that the line of the method results is very close to that of the X-plane simulated value. The green line is never more than 5m away from the original. For the vertical and horizontal speed, the values were also very close to the simulated values, usually within 0.1m/s accuracy. This simulation was performed under ideal conditions, without noise present, but it was concluded that the method is indeed capable of computing the aircraft state.

III. EXPERIMENT SETUP

In the previous chapter, the state finding method has been developed. Preliminary results from a simulation experiment indicate that the method can yield the desired results. After this, the algorithms were used in a flight test in the Netherlands. In this section, the experiment is described.

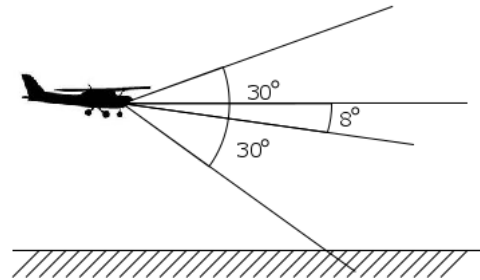


Figure 6: The aperture and direction of the radar, as mounted on the aircraft

The aircraft used is a Pipistrel Virus, and two freight containers are attached to the wings. In the front of one of the containers is the radar hardware. The radar antennas have a range of $3km$ and they are aimed to the front and downwards, such that they can always receive reflections from the track vector. The radar measurements are able to determine the range to a reflection accurate within $20m$, and the radial velocity is accurate to $0.3m/s$. An image of the aircraft can be seen in Figure 7, and the aperture and aim of the antenna are illustrated in Figure 6.



Figure 7: The test aircraft, with the radar in the front of the port freight container

The flight was performed on the 23rd of October 2019, under VMC. The location was the military airfield of Deelen, in the Netherlands, and the airspace was closed for other traffic. The pilot flew circuits around the airfield with increasing altitudes. The aircraft's true location and velocity were measured using an on-board GPS device. The flight was plotted in 3D using Google Earth, as seen in Figure 8.



Figure 8: The three-dimensional experiment flight path, containing circuits of increasing altitude

The FMCW radar was operational during the entire flight, including taxiing, similar to the GPS. Therefore, the radar state results are compared to the GPS track.

IV. RESULTS

The results of the experiment can be seen in Figure 9. The light green line in the background is the raw radar data, and it can be seen that high frequency variations are present. The first step in the computations is to apply outlier filtering and to discard data points of which the height differs by more than $150m$ from the GPS data. 15% of the data was removed in this manner.

The other data results are fed to a simple Kalman filter, to remove the variations of the signal [14]. Since the height and vertical speed are related to each other, the linear model for the filter used is:

$$x := Fx = \begin{bmatrix} 1 & 0 & 0 \\ 0 & 1 & 0 \\ 0 & -dt & 1 \end{bmatrix} \begin{bmatrix} V_x \\ V_z \\ h \end{bmatrix} \quad (8)$$

The negative sign in the equation is a consequence of V_z , being defined positive downward, which is the opposite direction of h , as was seen in Figure 3.

Similarly, it should be noted that the values for V_z in the second subfigure of Figure 9 are also positive downwards.

Kalman filtering does improve the accuracy of the results, as expected. Numerical values of the results are displayed in Table 1.

TABLE 1: NUMERIC RESULTS

| | Raw data | | Filtered results | |
|-------|------------|--------------------|------------------|--------------------|
| | Mean Error | Standard Deviation | Mean Error | Standard Deviation |
| V_x | $-0.42m/s$ | $6.36m/s$ | $-0.19m/s$ | $2.99m/s$ |
| V_z | $0.21m/s$ | $5.76m/s$ | $-0.13m/s$ | $1.98m/s$ |
| h | $36.27m$ | $36.83m$ | $36.57m$ | $23.82m$ |

From Table 1 it is seen that the estimates of the velocity have a small offset of several centimetres per second. The standard deviation is larger, in the order of several metres per second. It is also seen that the height measurements are on average $36m$ off, and that their standard deviation is of equal size.

The Kalman Filter removes high-frequency noise from the measurements and improves the results. The mean error of the velocity measurements becomes smaller and the standard deviation is reduced for all measurements.

Only the average difference in the altitude measurements does not improve when a Kalman filter is applied, but it is still around $36m$. This will be discussed further in the next section.

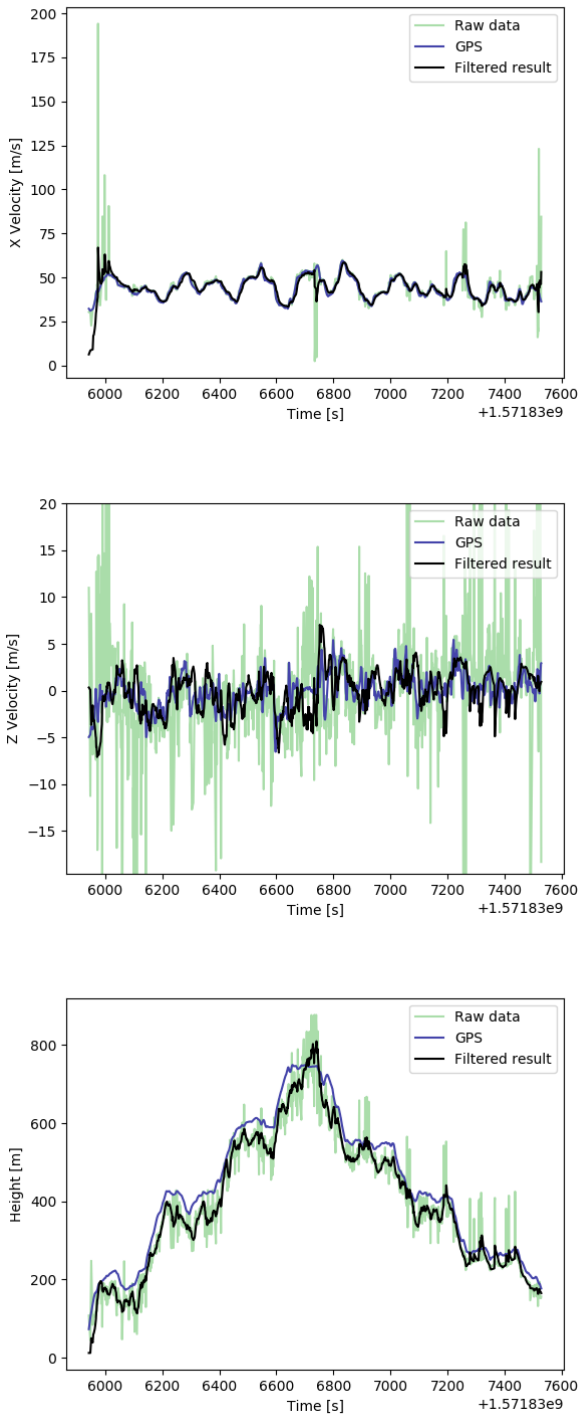


Figure 9: Radar, GPS and Filter results for the flight test

V. DISCUSSION

As noted above, the height difference between GPS and radar is on average $36m$ off. The origin of this is the difference in GPS altitude and terrain elevation. Whereas GPS computes the altitude above the earth model, the radar uses the reflections of the actual terrain. At the start of the flight, before take-off, the GSP indicated an altitude of $35.97m$. This explains why the radar has a mean error of about $36m$, or about $120ft$.

The height estimations are dependent on the position of the radar reflections. This means that trees and other foliage increase surface height, and therefore decrease the radar height further. The airport was surrounded by fields and forests, which cause variation. No official measurement of the tree height was available, but a four-story building on the airfield was just shorter than the treetops. Also, the airport is located in between several hills that are up to $25m$ higher than the runway. These can also have affected the height measurements. For a GA pilot concerned with avoiding ground collisions, the terrain height is far more important than the GPS altitude.

In Figure 9 it is seen that the V_x measurements are often very close to the actual speed, but that they are several times distorted by a few outliers which have not been removed by the first filter. These outliers affect the mean error and standard deviation, and their influence is reduced effectively by the Kalman filter.

Apart from the height difference, it is observed that the algorithm accuracy is similar to the performance of the hardware, of which the range accuracy is within $20m$ and the radial velocity accuracy is $0.3m$.

The vertical speed has more accurate results than the horizontal speed, which is a surprising since the radar was pointed to the front of the aircraft. This means that most of the reflections observed will lay in front of the aircraft, and therefore have a high horizontal radial velocity. It was therefore expected that the algorithm would be able to tell the horizontal velocity more accurately than the vertical velocity. The Kalman filter uses the relation between vertical speed and height, so extra information is available for a good estimate for both parameters.

A comparison is made between the accuracy of the radar results and those of conventional GPS navigation. GPS can determine the position of the sensor for 95% with a horizontal accuracy of $4m$, and vertically $8m$. The vertical accuracy of GPS is therefore better than that of the radar, but it should be noted that changes in the landscape such as areas of foliage are part of the radar variance.

Lastly, it should be noted that much space for improvement exists in the radar system. Better outlier filtering can have a significant impact on the V_x estimates, as well as the height

tracking. Increasing the measurement rate can be of great influence on the Kalman Filter results as well. This experiment was performed with one observation per second, but sampling rates of 10, 20 or 100 measurements per second are possible with modern day radar systems.

As mentioned in the Introduction, the availability and performance of modern microwave sensors and processors have increased significantly over the past years. In the last five years, the price of the equipment used in this experiment has decreased by a factor of 40, and the gain of available antennas has increased by over $10dB$. It is possible that the accuracy of the raw results of the radar system will surpass that of the GPS system in the next decade, for a similar price.

VI. CONCLUSION

In this paper, a novel strategy for altitude and velocity determination was presented. The algorithm is based on an on-board radar system and its reflections on the ground. It is therefore suitable for operations in the lower segments of the airspace, typically at altitudes used for General Aviation.

The system was tested in a local flight above relatively flat terrain. After a simple Kalman Filter was applied, velocity estimates have standard deviations of $2m/s$ or $3m/s$. Good outlier filtering is expected to improve these results significantly, such that the quality of the results approach those of navigation based on GPS.

Contrary to GPS however, the radar measures the distance to the surface height and is not dependent on a model of the earth. A fault in the GPS model resulted in a height error of $36m$, or $120ft$, which was not observed in the radar results.

The quality and price of available radar hardware has increased significantly in the past years. If this trend continues, it can be possible to bring a portable Collision Alert Radar on board of their aircraft. It is concluded that such a system can be used to detect ground speed and height information by performing direct measurements of the landscape.

Existing ground collision warning systems depend on an internal elevation model of the surface. This even applies to radio altimeters, who only measure directly below the aircraft. The Collision Alert Radar generates surface reflections in front of the aircraft, so it directly observes the terrain that is most relevant for the pilot. A radar system can therefore be a solution for pilots that do not wish to be dependent on the correctness of an elevation model.

REFERENCES

- [1] D. Nitti, F. Bovenga, M. Chiaradia, M. Grecco, G. Pinelli, "Feasibility of using synthetic aperture radar to aid UAV navigation", *Sensors*, vol. 15 issue 8, 2015, pp 13334-18359
- [2] M. Lee, Y. Kim, "Design and performance of a 24-GHz switch-antenna array FMCW radar system for automotive applications", *IEEE Transactions on Vehicular Technology*, vol 59, issue 5, 2010, pp 2290-2297
- [3] F. Folster, H. Rohling, U. Lubbert, "An automotive radar network based on 77GHz FMCW sensors", *IEEE national radar conference*, 2005, pp 871-876
- [4] R. Chavez-Garcia, O. Aycard, "Multiple sensor fusion and classification for moving object detection and tracking", *IEEE Transactions on Intelligent Transportation Systems*, Vol. 17, issue 2, 2015
- [5] J. Maas, R. Van Gent, J. Hoekstra, "Object tracking in images of an airborne wide angle FMCW radar", *Proceedings of International Conference for Research in Air Transportation*, 2018
- [6] A. G. Stove, "Linear FMCW radar techniques", *IEEE Proceedings for Radar and Signal Processing*, pp 343-350, 1992
- [7] C. Naulais, "General aviation radar system for navigation and attitude determination", *Delft University of Technology*, 2015
- [8] A. Meta, "Signal processing of FMCW synthetic aperture radar data", *Delft University of Technology*, 2006
- [9] J. Zhang, S. Wang, "An automated 2D multipass Doppler radar Velocity Dealiasing Scheme", *Journal of Atmospheric and Oceanic Technology*, vol. 23 issue 9, pp 1239-1248, 2006
- [10] S. Orfanidis, "Introduction to signal processing", *Pearson Education Inc*, 1972, ISBN0-13-209172-0
- [11] A. Weiss, B. Friedlander, "Eigenstructure methods for direction finding with sensor gain and phase uncertainties", *Circuits, Systems and Signal Processing*, vol. 9 issue 3, 1990
- [12] A. Shaw, "Improved wideband DOA estimation using modified TOPS algorithm", *IEEE Signal Processing Letters*, Vol. 23 Issue 12, 2016
- [13] D. Koks, "How to create and manipulate radar range-doppler plots", *Defence Science and Technology Organisation*, Edinburgh, Australia, December 2014
- [14] G. Welch, G. Bishop, "An Introduction to the Kalman Filter", *University of North Carolina at Chapel Hill*, 2001